BOUNDARY LAYER TRANSITION IN HIGH PRECISION CRITICAL NOZZLES OF VARIOUS SHAPES

Masahiro Ishibashi and Tatsuya Funaki
National Metrology Institute of Japan (AIST)
1-1-1 Umezono, Tsukuba-city, Ibaraki-prefecture, 305-8563 JAPAN
ishibashi.m@aist.go.jp

Abstract

Calibration results of accurately machined critical flow Venturi nozzles are summarized and a single fitted curve of the discharge coefficient against the Reynolds number were obtained that covers from the laminar to the turbulent boundary layer regimes. Possibility to use critical flow Venturi nozzles with smaller inlet curvature such as R=1.0D is discussed. Effects of diffuser length, inlet curvature, inlet diameter and inlet shape are also discussed. It is shown that theories will fail to predict discharge coefficient correctly when R is small.

Introduction

Reviewing the calibration results of accurately machined critical-flow Venturi nozzles (CFVNs) [1][2], the boundary layer transition in well machined CFVNs of typical geometry can be concluded to take place at the Reynolds number (R_e) between 1~2x10^6 as Stratford assumed [3]. It is possible to make a single fitted curve that will represent their discharge coefficient (C_d) at high accuracy in the whole R_e range from the laminar to the turbulent boundary layer regimes. The paper summarizes the past measurements using accurately machined CFVNs that relate to the boundary layer transition. Owing to the limited R_e range that the calibration facilities can reach, there are not enough C_d points of accurately machined CFVNs obtained in the turbulent boundary layer regime, so the paper uses the upper range of the Universal Curve proposed by Arnberg [4], which has been introduced in ISO/ASME standards [5][6] to represent C_d of normally machined CFVNs in the full R_e range. The paper also discuss a possibility to use nozzle geometries with a small inlet curvature to have a better performance.

Measurement of discharge coefficient

Unless otherwise noted, C_d was measured using a constant volume tank system or a closed-loop calibration facility developed as the middle-range air-flow national standard in Japan [7] that are shown in the picture. The calibrations were performed using dry air at room temperature at pressure of mainly 0.1~0.8 MPa but sometimes down to 10 kPa. All the C_d and R_e were calculated by the next equations that assume the ideal gas but the specific heat κ_0 was calculated at the upstream stagnation condition.

$$C_d = Q_{true}/Q_{theo} = Q_{true} \Big/ \frac{\pi D^2}{4}\sqrt{\left(\frac{2}{\kappa_0+1}\right)^{\frac{\kappa_0+1}{\kappa_0-1}}}\frac{P_0}{\sqrt{RT_0}} \quad (1)$$

$$R_e = 4Q_{true}/\pi D\mu_0 \quad (2)$$

When calibrating in the constant volume tank system, all the CFVNs were put in the nozzle holder shown in Fig. 1. When calibrating in the closed-loop calibration facility, a CFVN was put in a similar nozzle holder as Fig. 1 or directly put on a plate that has a 40 mmϕ hole to accept the CFVN, which was sandwiched between flanges of long straight 150A pipes. The CFVN was calibrated against a set of accurately machined critical nozzles.

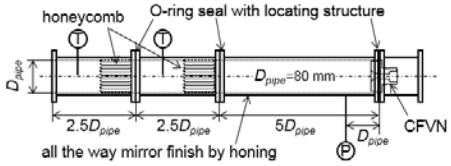

Fig. 1 The nozzle holder in the constant volume tank system

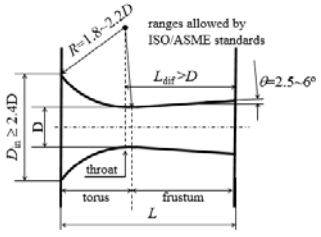

Fig. 2 The nomenclature and standards' values.

Discharge coefficient of BS-CFVN

Fig. 3 shows the measured C_d of the "Basic Shape (BS)" CFVNs, which have a toroidal throat of R=2D, D_{in}=2.5D, θ=3°, and L=4D, that comply with ISO/ASME standards. About the nomencrature, see Fig. 2. The standards' C_d curves for the normally machined and the accurately machined CFVNs are also plotted in the figure by the black solid lines, which are named in the paper as 'nCURVE' and 'aCURVE,' respectively. C_d of 18 accurately machined BS-CFVNs with D=9.7~18.9 mm were measured totally 2104 times in order to investigate the boundary layer trasition. The transition is clealy observed and concentrated at R_e=1~2x10^6. Assuming that C_d at the higher R_e obeys nCURVE and using the simoid function, C_d of BS-CFVNs can be fitted by a simple curve of eq. (3), which is named as 'sCURVE' in the paper and shown by the red solid line in the figure.

$$C_d^{\mathrm{sCURVE}} = \left(0.99845 - \frac{3.412}{\sqrt{R_D}}\right) - \left(0.00255 - \frac{0.692}{\sqrt{R_e}}\right)\frac{1}{1+\exp\left(19.3 - \frac{R_e}{7\times10^4}\right)} \qquad (3)$$

$$(2.4\times10^4 \le R_e \le 3.2\times10^7)$$

The maximum deviation of the measured C_d from sCURVE is abourt ±0.15% (see Fig. 4).

By the coutesy of Azbil Kimmon Co., Ltd., which is one of the JCSS accredited laboratories, C_d of 7 normally machined BS-CFVNs are shown in Fig. 5 [8][9]. These CFVNs (an example is shown in the picture) were very carefully machined by the company itself, with D=16.9~36.6 mm. Geometry of each nozzles was confirmed by a 3D co-ordinate machine in the order of 1 μm. Their C_d were measured using air in a closed loop calibration facility owned by the company. The reference meter was one of two G650 turbine flowmeters that are traceable to the national gas flow standard in Japan (the constant volume tank system in the picture) via accurately machined CFVNs. These turbine meters are so stable that there is no difference perceivable in the measured C_d depending on which turbine meter was used as the reference. By vitue of larger D, the measured C_d trace exactly along the sCURVE.

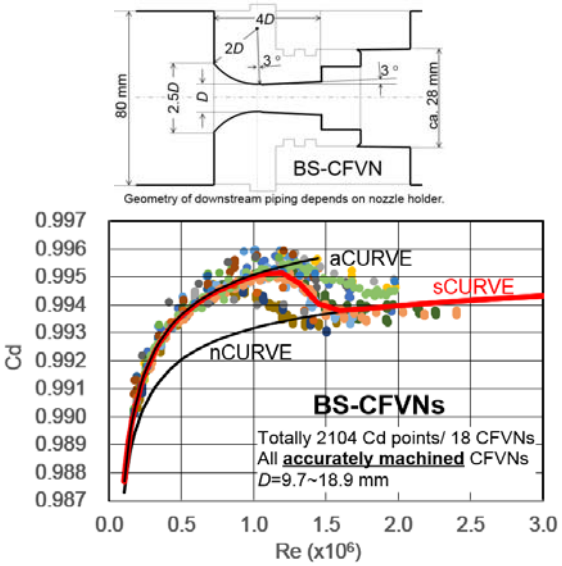

Fig. 3 C_d of accurately machined BS-CSVN.

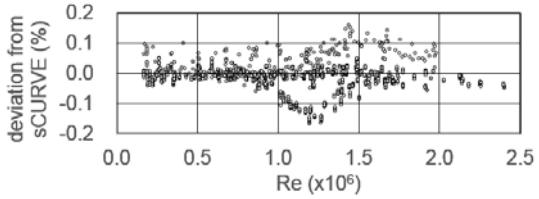

Fig. 4 Deviation of the measured C_d from sCURVE.

Example of accurately machined (left) and normally machined (right) CFVNs under measurements.

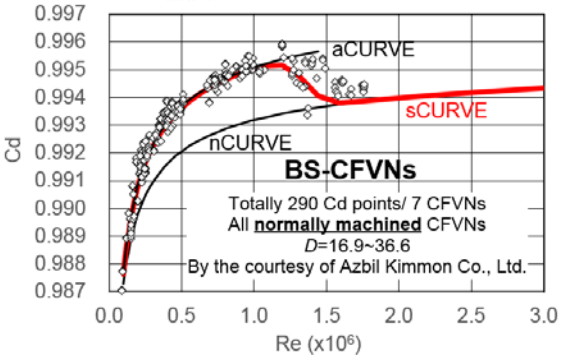

Fig. 5 C_d of normally machined BS-CSVNs.

Diffuser length

Fig. 6 shows C_d of a CFVN that does not comply with ISO/ASME standards but has the same C_d as BS-CFVN, which was categorized into 'nBbB-CFVN' and named as 'nBbB-CFVN-93degD.' It has a very short diffuser whose length is only 0.1D, but it has exactly the same C_d as BS-CFVN. It should be noted that the quadrant nozzle, that looks quite

similar to nBbB-CFVN-93degD but its nozzle exit is located exactly at the throat, will have somewhat different characteristics than BS-CFVN [10]. When the standards are to be revised, they can set down the diffuser length certainly shorter than the current value, which is longer than D, but excluding extremely short one.

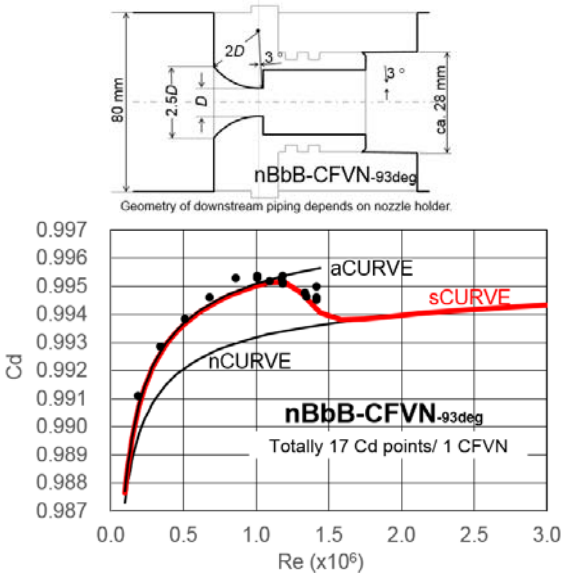

Fig. 6 Discharge coefficients of nBbB-CSVN.

Influence of upstream condition

The transition Re can be affected by certain geometry of CFVN or its holder. Fig. 7 shows C_d of an accurately machined CFVN, which has a quadrant inlet with D_{in}=5D with R=2D, categorized into 'QI-CFVN,' that showed no clear transition at Re up to 2x10^6. Currently, there is no data on other QI-CFVNs with R=2D, so the authors can not pinpoint the dominating factor that delayed the transition.

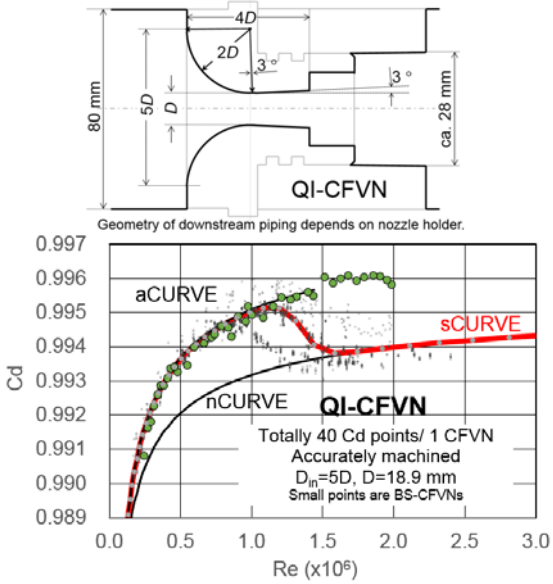

Fig. 7 Delayed transition in a QI-CFVN.

On the contrary, an obstacle on the upstream surface of BS-CFVN, that is categorized into 'oBS-CFVN,' had lowered the transtion Re as shown in Fig. 8 where C_d of a single accurately machined BS-CFVN with and without the obstacle are shown. This configulation is not complying with ISO/ASME standards but will be used later to force the transition take placwe at lower Re without changing the C_d in the laminar boundary layer regime. The transition path of the oBS-CFVN shown in Fig. 8 almost exactly coincides with the lowest transition path of BS-CFVNs shown in Fig. 3, therefore, this path may be able to be avoided by a careful use of CFVNs, then the error of eq.(3) will get smaller than that shown in FIg. 4.

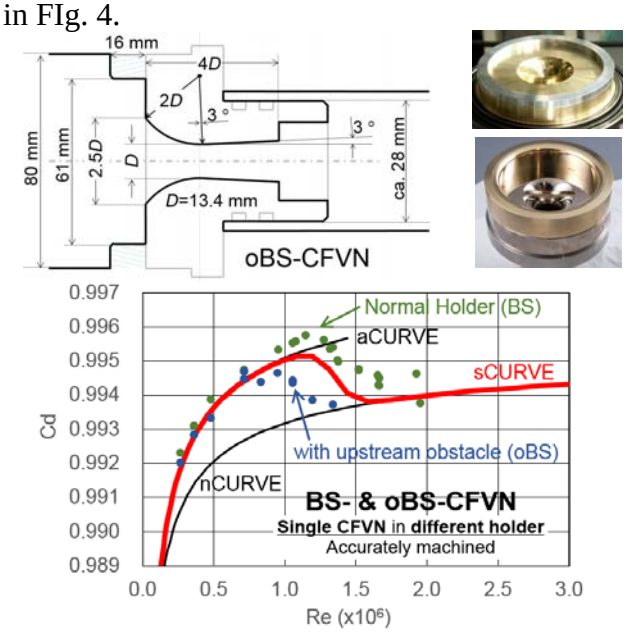

Fig. 8 Lowered transion by an upstream obstacle.

Possibility of R=1.0D CFVN as the new standard geometry

Stratford recommended to use CFVN that has R=2.0D inlet to minimize the C_d jump at the boundary layer transition, about which he assumed to take place at Re~10^6 [3]. He also estimated that the C_d jump by the transition will be in the order of 0.15%. His predictions agree very well with the measurements. However, he actually thought CFVNs of the smaller R would be more preferable because of the thinner boundary layer, but poor accuracy of theories to predict the laminar boundary layer thickness in such CFVNs made him abandon small R for absolute measurement. At that time, calibration of CFVN was not practical, so he had to use theoretical calculations. Actually for relative

measurement, he recommended even R=0.5D CFVN.

Nowadays, situation has been changed, that is, we can calibrate CFVNs very precisely in wide R_e range, so we have a potential to look for another geometry for better performance.

Fig. 9 shows the predictions of C_d of R=2.0D and R=1.0D CFVNs by Stratford and depicts the boundary layer transitions. In CFVNs of smaller R, the boundary layer thickness is thinner thus the jump of C_d should be smaller. The dependence of C_d on R_e in the turbulent boundary layer regime is also smaller in smaller R CFVNs. C_d of smaller R CFVN is certainly smaller but it is caused by the 2D core flow that is constant all the way at any R_e. From the viewpoint of machining a nozzle, CFVN with smaller R has certain advantages because of the shorter length, but too small R will introduce difficulty in machining and geometry error will affect more significantly to the flow characteristics, so there must be an adequate range of R. There are no crucial disadvantages in smaller R CFVNs if it can be machined with sufficiently small scattering.

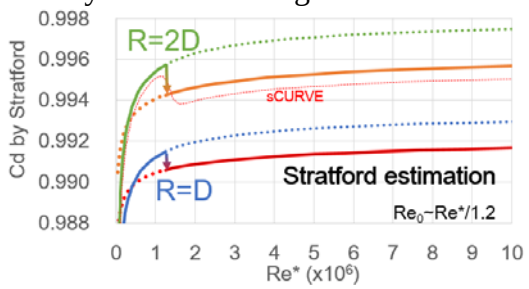

Fig. 9 C_d predicedby Stratford.

Fig. 10 shows the measured C_d of 5 accurately machined CFVNs with R=1.0D inlet. Three of them had D_{in}=2.5D otherwise D_{in}=3.0D (QI-CFVN). They were named as 'R10D-CFVN.' Their throat diameters were from 9.5 to 18.9 mm. In the lowest R_e range, C_d were measured against another accurately machined CFVN connected in series [11].

There is no boundary transition observed in the measuring range, therefore, a simple and traditional fitted curve was obtained that is named as 'bCURVE.'

$$C_d^{\,\mathrm{bCURVE}} = 0.9961 - \frac{2.781}{\sqrt{R_e}} \qquad (4)$$

$$(1.5\times10^4 \le R_e \le 2.0\times10^6)$$

Surprisingly, it exactly coincides with the nCURVE. It should be pointed out that Stratford and so as Geropp-Hall [12] failed to predict C_d of R=1.0D CFVNs.

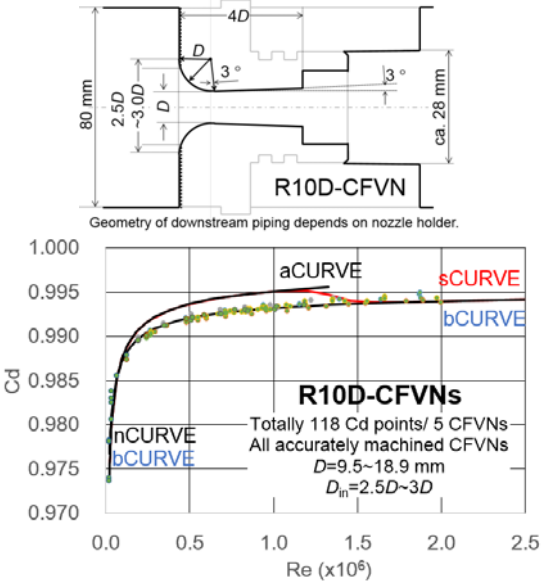

Fig. 10 C_d of R10D-CFVNs.

To look into the details, Fig. 10 is magnified in Fig. 11. Scattering of C_d is in the same level as BS-CFVN. The larger accelaration on front of the throat may have delayed the transition. In that case, there will be an unrevealed jump at R_e>2x10^6, however, it should be smaller than that in sCURVE as seen in Fig. 9. A seamless characteristics from the laminar to the turbulent boundary layer regimes is still one of the possibilities. According to what measured up to now, R10D-CFVN has a potential to replace the standard CFVN geometry to have a better performance.

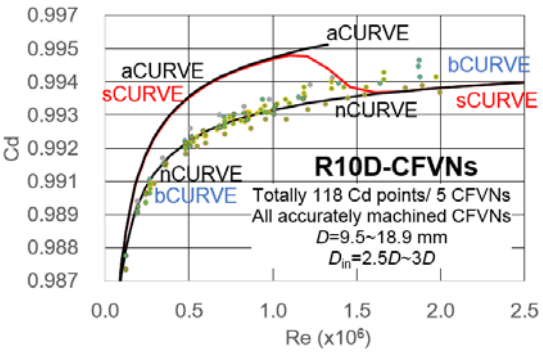

Fig. 11 C_d of R=1.0D CFVNs (magnified).

Influence of the inlet curvature *R*

Effect of the inlet curvatures is summarized in Fig. 12, which shows the fitted curves based on totally 264 measured C_d using 8 accurately machined CFVNs with various R (named as 'R%%D-CFVN' where %% is the number R/Dx10). All the R%%D-CFVNs have the quadrant inlet except for three R10D-

CFVNs, in which D_{in}=2.5D. It is confirmed from the fitted curves that the smaller R is, the smaller sensitivity of C_d on R_e is, that is an advantage of smaller R CFVNs. The differences betwen the curves of R12D~R25D-CFVNs are within the scattering of the calibration facility, therefore, the limits of R in ISO/ASME standards, which is 1.8D~2.2D, is reasonable but can be widened slightly if necessary. It was also observed that the Stratford and the Geropp-Hall theories can not estimate the shift of C_d at small R as shown in Fig. 13.

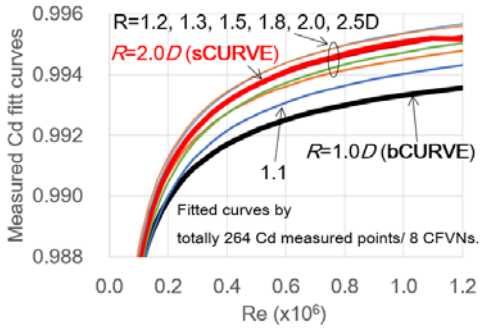

Fig. 12 Measured fitted curves of CFVNs of various inlet curvature R.

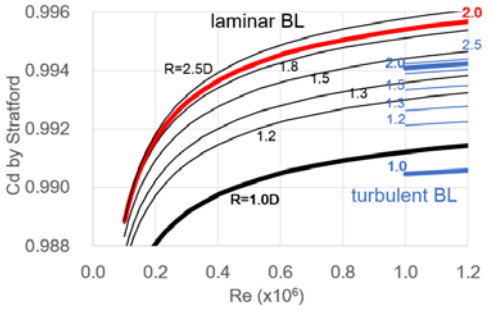

Fig. 13 Prediction by Stratford.

The measured C_d of each R%%D-CFVNs are shown in Figs. 14 in which some interesting phenomena are observed. R25D-CFVN does not have the transition obeying sCURVE, however, R18D-CFVN does. R15D-CFVNs also don't have the transition along sCURVE. These scattering of the phenomenon is confusing, but the authors guess that it may be affected by the distance from the nozzle holder wall to the starting point of the inlet contraction, that is, in the larger R CFVNs, the distance dominates but in the smaller R CFVNs, the transition is delayed simply by the larger preferable pressure distribution. The red points in the figures were measured with the obstacle shown in Fig. 7 that should lower the transition R_e. In a R15D-CFVN, it was succeeded but not in R12D- and R11D-CFVNs, that should be because of the stronger boundary layer in small R CFVNs.

R08D- and R05D-CFVNs also act as normal CFVNs as shown in the last figure of Figs. 14, however, for the practical applications, the difficulty to machine very small curvature with small scattering should be taken into consideration.

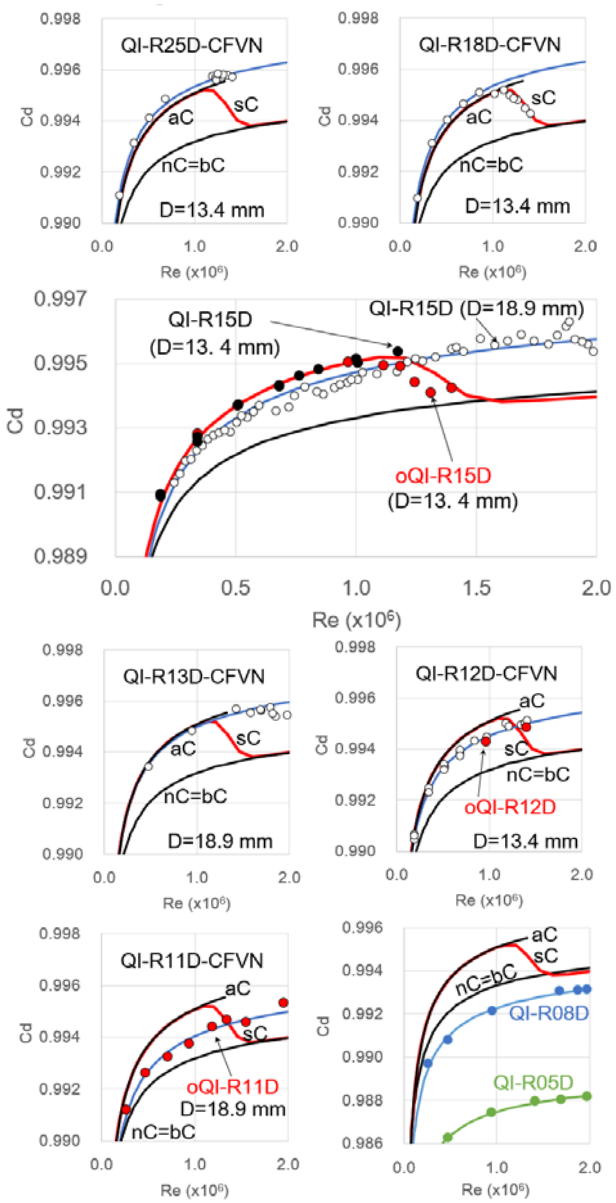

Figs. 14 C_d of R%%D-CFVNs. Red points were measured with an obstacle shown in Fig. 7.

Influence of the inlet diameter D_{in}

The inlet plane of one of QI-BS-CFVNs with D=13.4 mm was shaved to have "free-standing lip' or 'flat inlet' shapes as shown in Fig. 15. They were categorized into 'FI-CFVN' and 'FSL-CFVN,' respectively. Each of the FSL-CFVNs were named as 'T%-CFVNs' as shown in Fig. 16. After being shaved to be a FSL-CFVN, its free-standing lip was then

covered by an adequate ring to be a FI-CFVN, that was named as 'T%r-CFVN.' Two frustums were also tested to recover a long inlet contraction as in Fig. 15.

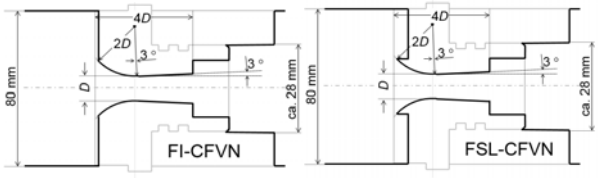

Shaved CFVN with "Flat Inlet. Shaved CFVN with "Free-Standing Lip."

Fig. 15 CFVNs under measurement.

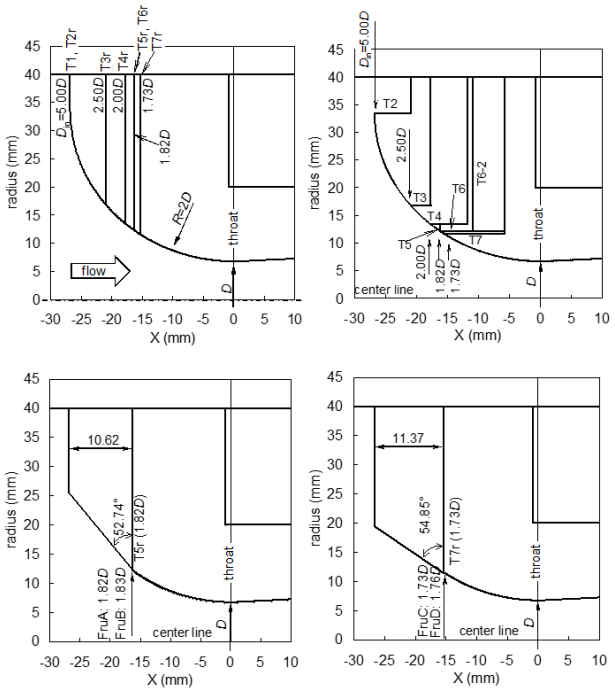

Fig. 16 CFVNs under measurement.

Figs. 18 show the measured C_d of T%- and T%r-CFVNs. There were no change detected in C_d till the nozzle was shaved to be T4 that is FSL-CFVN with D_{in}=2.0D. T4r still have the initial C_d, therefore, the range for D_{in} allowed in ISO/ASME standards, which is D_{in}>2.4D, is reasonable. When the inlet was shaved down to D_{in} =1.82D, a frustum is needed to recover the initial C_d. The frustum is effective for a certain smaller D_{in}, but C_d is getting sensitive to the shape of the frustum.

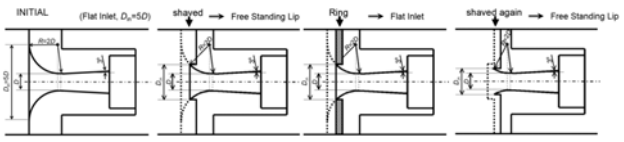

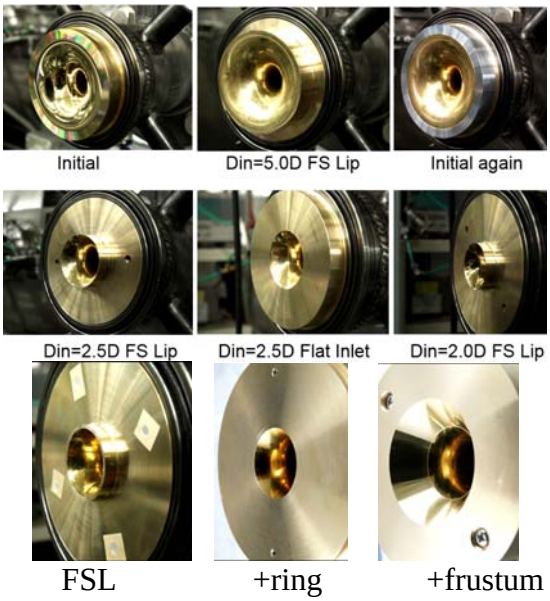

FSL +ring +frustum

Fig. 17 Examples of FI- and FSL-CFVNs.

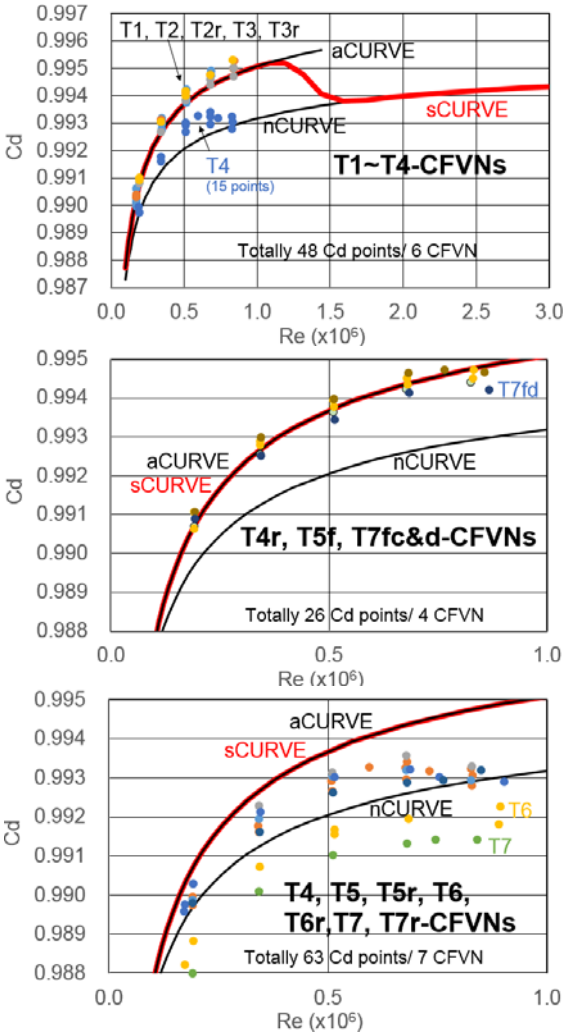

Fig. 18 C_d of T%-CFVNs.

Conclusions

Reviewing the calibration results of 18 accurately machined critical flow Venturi nozzles with a similar shape, the boundary layer transition was clearly observed in the measured

discharge coefficients at the Reynolds numbers between 1×10^6 to 2×10^6. Using more than 2000 measured discharge coefficients and the standard curve in the turbulent boundary layer regime, a single fitted curve expressed by a simple function was obtained that covered from the laminar to the turbulent boundary layer regimes. The maximum deviation of the measured discharge coefficients from the fitted curve was ±0.15%. It was also shown that the discharge coefficients of 8 normally machined critical flow Venturi nozzles exactly traced on the fitted curve including the boundary layer transition regime.

Use of critical flow Venturi nozzles with a smaller inlet curvature R such as R=1.0D was discussed. Calibration results of 5 accurately machined critical flow Venturi nozzles with R=1.0D showed stable discharge coefficients in wide Reynolds number range at the same level as the standard geometry nozzles with R=2.0D, however, the boundary layer transition was not observed in the measuring Reynolds number up to 2×10^6, that was considered to be resulted in by the stronger preferable pressure distribution on front of the throat. Critical flow Venturi nozzles of various inlet curvature from 0.5D to 2.5D were calibrated. It was shown that theories failed to predict discharge coefficient at smaller R.

Effects of diffuser length, inlet curvature, inlet diameter and inlet shape were also investigated. The allowed geometry ranges in the standards for inlet diameter and inlet curvature were considered to be reasonable, but it was shown that certainly shorter diffuser length should be allowed.

Acknowledgement

The authors would like to express their sincere thanks to Mr. Thomas B. Arnberg for valuable and comprehensive discussions on CFVNs and also for motivating many kinds of research works. The authors also would like to thank Calibration Service Center of Azbil Kimmon Co., Ltd. for kindly offering the calibration data on its normally machined CFVNs.

References

[1] M. Ishibashi et al., "Discharge coefficient of super-accurate critical nozzles accompanied with the boundary layer transition measured by reference super-accurate critical nozzles connected in series," Proceedings of ASME FEDSM'01, Paper No. 18036, New Orleans, 29 May-1 June 2001.

[2] M. Ishibashi, "Fluid dynamics in critical nozzles revealed by measurements," Proceedings of FEDSM'03, Paper No. 45592, Honolulu, July 6-11, 2003.

[3] B. T. Arnberg et al.,"Discharge coefficient equations for critical-flow toroidal-throat Venturi nozzles," Proceedings of ASME FEDSM'01, Paper No. 18030, New Orleans, May 29-June 1, 2001.

[4] B. S. Stratford, "The Calculation of the Discharge Coefficient of Profiled Choked Nozzles and the Optimum Profile for Absolute Air Flow Measurement," Journal of the Royal Aeronautical Society, Vol. 58, pp. 237-245, 1964.

[5] ISO 9300: 2005, "Measurement of gas flow by means of critical flow Venturi nozzles."

[6] ASME PTC 19.5-2004, "Flow Measurement."

[7] M. Ishibashi et al., "The renewed airflow standard system in Japan for 5-1000 m3/h," Flow Measurement and Instrumentation, Vol. 17, pp. 153-161, 2006.

[8] H. Inanaga et al.,"Practical calibration method of Sonic nozzles (in Japanese)," Proceedings of SICE 2000, July 26-28, 2000.

[9] H. Inanaga et al.,"Gas meter calibration system using sonic nozzles as reference standards," Proceedings of NCSL 2000, November 22, Tokyo.

10] M. Ishibashi et al., "Discharge coefficients of critical nozzles with step near the throat and their flow field estimated from recovery temperature distribution," Proceeding of ASDME FEDSM'01, Paper No. 18035, New Orleans, May 29-June 1, 2001.

[11] M. Ishibashi et al., "Methods to calibrate a critical nozzle and flowmeter using reference critical nozzles," Flow Measurement and Instrumentation, Vo. 11, pp. 293-303, 2000.

[12] M. Ishibashi et al.,"Theoretical discharge coefficient of a critical circular-arc nozzle with laminar boundary layer and its verification by measurements using super-accurate nozzles," Flow Measurement and Instrumentation, Vol. 11, pp.305-313, 2000.